

# SPACE-TIME DESIGN FOR DEEP JOINT SOURCE CHANNEL CODING OF IMAGES OVER MIMO CHANNELS

Chenghong Bian, Yulin Shao, Haotian Wu, Deniz Gündüz

Department of Electrical and Electronic Engineering, Imperial College London

## ABSTRACT

We propose novel deep joint source-channel coding (DeepJSCC) algorithms for wireless image transmission over multi-input multi-output (MIMO) Rayleigh fading channels, when channel state information (CSI) is available only at the receiver. We consider two different transmission schemes; one exploiting spatial diversity and the other one exploiting spatial multiplexing of the MIMO channel. In the diversity scheme, we utilize an orthogonal space-time block code (OSTBC) to achieve full diversity which increases the robustness of transmission against channel variations. The multiplexing scheme, on the other hand, allows the user to directly map the code-word to the antennas, where the additional degree-of-freedom is used to send more information about the source signal. Simulation results show that the diversity scheme outperforms the multiplexing scheme at lower signal-to-noise ratio (SNR) values and smaller number of receive antennas at the AP. When the number of transmit antennas is greater than two, however, the full-diversity scheme becomes less beneficial. We also show that both the diversity and multiplexing scheme can achieve comparable performance with the state-of-the-art BPG algorithm delivered at the MIMO capacity in the considered scenarios.

**Index Terms**— deep joint source-channel coding, orthogonal space-time block codes, diversity-multiplexing trade-off

## 1. INTRODUCTION

Shannon’s separation theorem states that separate source and channel coding is optimal at the infinite block length asymptotic. However, practical systems are limited to finite block lengths, in which case, separation can be highly sub-optimal. Over the years, researchers have designed various joint source and channel coding (JSCC) algorithms to improve the reconstruction performance at the receiver [1]. However, due to the higher complexity and difficulty in designing such codes, separation-based schemes are still widely used. Recently, due to the increasing interest in augmented and virtual reality (AR/VR) systems and other latency-constrained edge applications, JSCC schemes are receiving growing interest, also under the framework of semantic communications [2].

Deep learning with deep neural networks (DNN) have also found applications in various communication problems [3–5], including compression [6, 7] and channel coding [8–10]. The



**Fig. 1:** System Model. STM denotes the space-time mapping block and Det represents the equalization/detection block.

lack of high-performing practical JSCC schemes also motivated research on deep learning aided JSCC schemes over the last years [11–14]. In [11], the authors proposed the first deep learning based JSCC scheme called DeepJSCC for wireless image transmission, and showed that it achieves comparable performance with the separation schemes while avoiding the cliff-effect. DeepJSCC is later extended to the channels with feedback in [12], and to multipath fading channels in [13, 15]. All of these works illustrate the effectiveness of DeepJSCC as a promising technology for next-generation communication systems.

JSCC over block-fading multiple-input multiple-output (MIMO) channels is studied in [16] from an information-theoretic perspective, focusing on the high signal-to-noise ratio (SNR) regime. The authors proposed a layered transmission scheme, and showed that each layer should operate on a different point at the diversity-multiplexing trade-off [17]. This analysis is later extended to the finite SNR regime in [18]. However, the analysis in both of these papers are mainly theoretical focusing on Gaussian sources.

In this paper, our goal is to design JSCC schemes for practical wireless image transmission over MIMO fading channels. In particular, we consider a multi-antenna transmitter-receiver pair, and study two schemes for image delivery using DeepJSCC. For *diversity scheme*, the transmitter generates the latent vector, which is then mapped to the antennas according to OSTBC designs. With perfect channel state information (CSI), the receiver can decouple the received signals at its antennas and achieve full-diversity. This introduces redundancy, and increases the robustness of the transmitted symbols against channel variations. For the multiplexing scheme, the user directly maps the latent vector to the antennas while the AP first equalizes the received signal using residual-assisted [13, 19] minimum mean square error (MMSE) equalizer and then reconstructs the image. We note that the multiplexing scheme is more general, and in principle, the DeepJSCC encoder/decoder pair, trained in an end-to-end fashion, can learn to introduce redun-

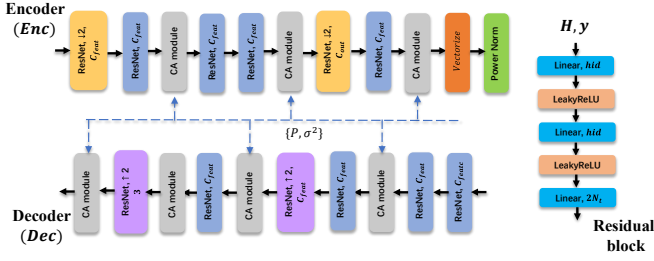


**Fig. 2:** The structure of the encoder (top), decoder (bottom), and the residual block for MIMO equalization at the AP (right). The CA modules take the features, the signal power,  $P$ , and the noise power  $\sigma^2$  as input.  $hid$  denotes the number of hidden neurons in the residual block.

dancy against channel variations when necessary (e.g., in the low SNR regime). Our goal here is to investigate whether introducing such domain knowledge into the DeepJSCC architecture can help the system to achieve a better performance. Simulation results confirm the benefits of this approach in the low SNR regime which highlights the importance of domain knowledge and model-based design when incorporating deep learning technique into the design of future communication system. Simulation results also reveal the comparable performance of the proposed schemes to the separation scheme using BPG algorithm with instantaneous MIMO capacity which is a rather loose upper bound on the performance of any separation-based scheme employing BPG for compression.

## 2. PROBLEM FORMULATION

We consider a communication system where a user tries to transmit an image to an access point (AP) over Rayleigh fading MIMO channel, as illustrated in Fig. 1. We assume that the user is equipped with  $N_t$  antennas while the AP has  $N_r$  antennas.

Denote by  $\mathbf{X} \in \mathbb{R}^{C \times H \times W}$  the image at the user, where  $C$ ,  $H$  and  $W$  are the number of color channels, height, and width of the image. The transmitter transforms  $\mathbf{X}$  into a matrix  $\mathbf{S} \in \mathbb{C}^{N_t \times k}$  with  $\|\mathbf{S}\|_F^2 \leq N_t k$ , where  $k$  denotes the number of channel uses. We define the *bandwidth ratio*,  $\rho$ , as the number of channel uses per pixel, i.e.,  $\rho \triangleq k/(CHW)$ . Finally, given the power constraint  $P$  at each transmit antenna,  $\mathbf{S}$  is scaled to  $\sqrt{P}\mathbf{S}$  before transmission.

We assume a block Rayleigh fading channel between the user and the AP, where the channel remains constant during the transmission of each image. The channel state is denoted by  $\mathbf{H} \in \mathbb{C}^{N_r \times N_t}$ , where each element follows complex Gaussian distribution with zero-mean and unit-variance. Therefore, the received signal at the AP can be written as

$$\mathbf{Y} = \sqrt{P}\mathbf{H}\mathbf{S} + \mathbf{N}, \quad (1)$$

where  $\mathbf{Y} \in \mathbb{C}^{N_r \times k}$  and  $\mathbf{N} \in \mathbb{C}^{N_r \times k}$  denotes the complex additive white Gaussian noise (AWGN) at the AP, following

$N_{ij} \sim \mathcal{CN}(0, \sigma^2)$ . We define the average SNR as:

$$SNR \triangleq \frac{P}{N_t \sigma^2}, \quad (2)$$

where  $N_t$  in the denominator ensures that the average SNR at each receive antenna remains constant with different number of transmit antennas. We assume that the receiver has perfect CSI while the transmitter does not. Thus, given  $\mathbf{Y}$ , the AP first generates an estimate of  $\mathbf{S}$ , and then reconstructs the original image based on this estimate. The goal is to minimize the loss between the original image and the reconstructed one, which will be introduced in the subsequent section.

## 3. DEEPJSCC OVER A MIMO CHANNEL

For the proposed DeepJSCC methods, the user first encodes  $\mathbf{X}$  by the DeepJSCC encoder, denoted by Enc, and obtain the latent vector  $\mathbf{z} \in \mathbb{C}^l$  which is normalized as:

$$\mathbb{E}\|\mathbf{z}\|_2^2 \leq l \quad (3)$$

where  $l$  denotes the number of complex symbols employed to encode the image before mapping to the antennas.

Before transmission, the transmitter applies a space-time mapping, denoted by STM, to the normalized vector. STM can be either a space-time coding scheme in order to achieve diversity gain, or an identical mapping to achieve multiplexing gain. We denote by  $\mathbf{s}$  the output of STM at the user which is then loaded to  $N_t$  antennas sequentially and scaled to form the transmitted signal  $\sqrt{P}\mathbf{S}$ . After passing the channel as in (1), an estimate of the latent vector, denoted by  $\tilde{\mathbf{z}}$ , is generated based on the received signal  $\mathbf{Y}$  and the CSI,  $\mathbf{H}$ . Then the reconstructed image can be expressed as  $\tilde{\mathbf{X}} = \text{Dec}(\tilde{\mathbf{z}})$ , where Dec stands for the neural decoder function. The mean squared error (MSE) loss is adopted to measure the reconstruction error, expressed as:  $\mathcal{L}(\text{Enc}, \text{Dec}) = \mathbb{E}\|\mathbf{X} - \tilde{\mathbf{X}}\|_F^2$ .

The encoder (Enc) and decoder (Dec) structures are shown in Fig. 2, where the pixel shuffling [20] is used inside the module ‘ResNet,  $\uparrow 2$ ’ to upsample the input features. Note that we also add the channel attention (CA) modules [21], which takes  $P$  and  $\sigma^2$  as input in both Enc and Dec to ensure that the system is robust to different SNR regimes. It is well-known that multiple antennas can provide both diversity and multiplexing gain [17]. In separation-based approaches different space-time codes [22, 23] can be exploited to operate on different points of the trade-off between the diversity and multiplexing gains in a MIMO channel. Here, our goal is to explore whether such schemes can also benefit the DeepJSCC approach by explicitly introducing structures into the code design. We will introduce two distinct transmission strategies to achieve this, and explore whether an explicit diversity scheme can be beneficial to achieve a more robust DeepJSCC performance especially in the low SNR regime.

### 3.1. Full Diversity Transmission

The first scheme aims to achieve full diversity via OSTBC [22]. We first consider the user has two transmit antennas; and

hence, the well-known Alamouti scheme [24] is used. The space-time mapping STM for the Alamouti scheme is described as follows: we group the latent vector  $\mathbf{z}$  into pairs:  $\mathbf{z} = \{\{z_1, z_2\}, \dots, \{z_{k-1}, z_k\}\}^1$ , and STM is performed separately on each pair. Consider, for example, the first pair  $\{z_1, z_2\}$ , where the first antenna, transmits  $s_A[1] = \sqrt{P}z_1$  and  $s_A[2] = -\sqrt{P}z_2^*$  in the first and second time slots, while the second antenna, transmits  $s_B[1] = \sqrt{P}z_2$  and  $s_B[2] = \sqrt{P}z_1^*$ . According to (1), the received signals in the first two time slots can be written as:

$$\begin{aligned} \mathbf{y}_1 &= \sqrt{P}\mathbf{H}[z_1, z_2]^\top + \mathbf{n}_1, \\ \mathbf{y}_2 &= \sqrt{P}\mathbf{H}[-z_2^*, z_1^*]^\top + \mathbf{n}_2, \end{aligned} \quad (4)$$

where the subscripts for  $\mathbf{y}$  denotes the index of the time slot. According to [24], we can decouple  $z_1, z_2$  from (4) as:

$$\begin{aligned} \hat{m}_1 &= \sqrt{P}\mathbf{h}_A^H \mathbf{y}_1 + \sqrt{P}\mathbf{y}_2^H \mathbf{h}_B, \\ \hat{m}_2 &= \sqrt{P}\mathbf{h}_B^H \mathbf{y}_1 - \sqrt{P}\mathbf{y}_2^H \mathbf{h}_A, \end{aligned} \quad (5)$$

where  $\mathbf{h}_A, \mathbf{h}_B$  are the first and second columns of  $\mathbf{H}$ , and  $\hat{m}_1, \hat{m}_2$  are intermediate variables. By substituting the expression of  $\mathbf{y}_1, \mathbf{y}_2$  into (5), and apply the MMSE estimator to  $\hat{m}_1$  and  $\hat{m}_2$ , the estimated  $\hat{z}_1, \hat{z}_2$  are obtained as:

$$\begin{aligned} \hat{z}_1 &= \hat{m}_1 / [P(\|\mathbf{h}_A\|_2^2 + \|\mathbf{h}_B\|_2^2) + \sigma^2], \\ \hat{z}_2 &= \hat{m}_2 / [P(\|\mathbf{h}_A\|_2^2 + \|\mathbf{h}_B\|_2^2) + \sigma^2]. \end{aligned} \quad (6)$$

We can then apply the same algorithm to estimate the remaining pairs  $\{\hat{z}_{2i-1}, \hat{z}_{2i}\}, i \in [2, k/2]$ . Then the estimated sequence  $\hat{\mathbf{z}}$  is fed to the subsequent source decoder Dec to reconstruct the image  $\hat{\mathbf{X}}$ .

We also consider the system with three transmit antennas. Note that when  $N_t > 2$ , the rate-1 space time code that achieves full diversity does not exist, and we will adopt two OSTBC designs with rates 1/2 and 3/4, respectively. Since these codes belong to the class of *generalized complex orthogonal designs*, we can estimate the transmitted symbols  $\mathbf{z}$  similar to that in (6). Due to the page limit, we refer the interested readers to [22] for a detailed explanation of the design and the corresponding decoding algorithm for these codes.

### 3.2. Multiplexing Scheme

Previous scheme utilizes the OSTBC to exploit the diversity of the MIMO system; however, the orthogonal designs transmit  $K$  symbols using  $N \geq K$  channel uses causing a rate loss which may hinder the system performance when the channel quality improves. Thus, we design a new strategy, called the multiplexing scheme, where  $N_t N$  symbols are transmitted in  $N$  channel uses. The STM output  $\mathbf{s}$  is identical to the unit-variance latent vector  $\mathbf{z}$  and the transmitter simply reshapes  $\mathbf{z}$  to a matrix,  $\mathbf{Z} \in \mathcal{C}^{N_t \times k}$ , and the final transmitted signal is  $\mathbf{S} = \sqrt{P}\mathbf{Z}$ .

After passing the channel, the AP estimates  $\mathbf{Z}[i], i \in [1, k]$ , given  $\mathbf{Y}[i]$  and  $\mathbf{H}$ . In traditional digital systems, the latent

<sup>1</sup>Note that  $\mathbf{z}$  can be zero-padded if the length of it is odd.

vector  $\mathbf{Z}[i]$  is comprised of QAM symbols and sphere decoding can be used [25]. However, the transmitted symbols are not constrained to a finite constellation; thus, we adopt MMSE equalization to first generate a coarse estimation, which is expressed as:

$$\mathbf{Z}_{MMSE}[i] = \mathbf{H}^H (\mathbf{H}\mathbf{H}^H + \frac{\sigma^2}{P} \mathbf{I}_{N_r})^{-1} \mathbf{Y}[i]. \quad (7)$$

Motivated by [19], we add a residual connection layer, denoted by Res, to calibrate the estimation error of (7) as shown in Fig. 2. The Res layer takes the concatenated real-valued  $\mathbf{Y}[i]$  and  $\mathbf{H}$  as input and the final estimation is given by:

$$\hat{\mathbf{Z}}[i] = \mathbf{Z}_{MMSE}[i] + \text{Res}(\mathbf{Y}[i], \mathbf{H}). \quad (8)$$

Note that  $\hat{\mathbf{Z}}$  is vectorized and fed to the subsequent decoder Dec for reconstruction. Both schemes are trained in an end-to-end manner in order to minimize the MSE between the input and output images.

## 4. EXPERIMENTS

### 4.1. Training and implementation details

We evaluate the proposed diversity and multiplexing schemes<sup>2</sup> for the transmission of images from the CIFAR-10 dataset, which consists of 50000 training and 10000 test RGB images, each with  $32 \times 32$  resolution. The number of neurons in the Res block, denoted by *hid* is set to 128. The Adam optimizer is used. Learning rate is initialized at  $10^{-4}$ , and is reduced by a factor of 0.8 if the validation loss does not drop in 4 consecutive epochs. Early stopping is used, where the training process will terminate when the validation loss does not drop over 12 epochs. The number of maximum training epochs is set to 400. We only study the cases with  $N_t = 2, 3$  and  $N_r = 1, 2, 4$ .

### 4.2. Results

We will compare the proposed DeepJSCC approaches with a separation-based ideal benchmark, where we will assume that the transmitter knows the instantaneous channel capacity<sup>3</sup> that could be achieved at each channel block, given by:

$$C(\mathbf{H}) = \log_2(\det(\mathbf{I}_2 + \frac{P}{\sigma^2} \mathbf{H}^H \mathbf{H})). \quad (9)$$

We then evaluate the PSNR achieved at the AP when BPG compression is used for compressing the image at the rate imposed by  $C(\mathbf{H})$ , and averaged these over the dataset.

We first compare the performance of the two schemes with the benchmark in Fig. 3 for  $N_t = 2, N_r \in \{1, 2, 4\}$  and bandwidth ratio  $\rho = 1/8$ . We highlight that the CA modules introduced in Sec. 3 are used to adapt to different SNR regimes

<sup>2</sup>To reproduce the results, we make the source code publicly available at [https://github.com/aprilbian/ST\\_JSCC](https://github.com/aprilbian/ST_JSCC).

<sup>3</sup>Note that in practice, the transmitter does not know the channel capacity, thus it should compress the image at a lower rate to avoid outage [18].

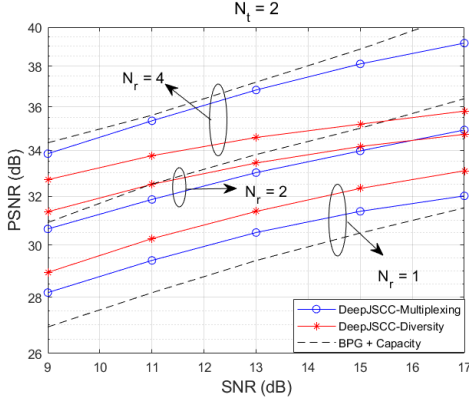


**Fig. 3:** The PSNR performance for the proposed schemes and the digital baseline with  $N_t = 2$ ,  $N_r \in \{1, 2, 4\}$ .

ranging from 9 dB to 17 dB. As can be seen from the figure, for different number of receive antennas, the relative performance between the diversity and multiplexing schemes changes. To be specific, when  $N_r = 1$ , the diversity scheme is much better than the multiplexing scheme even in the high SNR regime. For  $N_r = 2$ , the multiplexing scheme outperforms the diversity scheme when  $SNR > 16$  dB. For  $N_r = 4$ , the multiplexing scheme is superior at all SNR regimes. These results are aligned with those in [16], where it is shown that the optimal multiplexing gain increases when the system has more number of antennas, or equivalently, a better diversity-multiplexing trade-off. The intuition is that, when the SNR is low, diversity is more beneficial as it increases the reliability of transmission. However, as the SNR increases, since reliability is warranted, it becomes more beneficial to exploit the transmit antennas for multiplexing to reduce the end-to-end distortion.

We also observe that the DeepJSCC schemes outperform the separation-based benchmark at all SNR regimes when  $N_r = 1$ . For  $N_r = 2$ , they are outperformed at higher SNR values and the benchmark always maintains a PSNR gain compared to the learned schemes with  $N_r = 4$ . We note that the MIMO capacity  $C(\mathbf{H})$  shown in (9) increases rapidly with  $N_r$ , yet it is unachievable with a finite block length. On the other hand, it is remarkable that the proposed DeepJSCC schemes can outperform this idealized upper bound on separation performance in the low SNR and limited receive antenna scenarios. We note that this is aligned with previous results on DeepJSCC [11], where it has been observed to provide major gains in the low SNR and low bandwidth ratio regimes. When used for multiplexing gain, multiple antennas effectively increase the available channel bandwidth.

Finally, we present the comparison of the diversity and the multiplexing schemes with  $N_t = 3$  antennas and a single receive antenna ( $N_r = 1$ ) in Fig. 4. Two OSTBC designs are evaluated. All three models are trained and tested under  $SNR \in [2, 10]$  dB. When  $\rho = 1/8$ , even in the low SNR regime, both diversity schemes are outperformed by the multiplexing scheme. This can be explained by the fact that OSTBC rate for

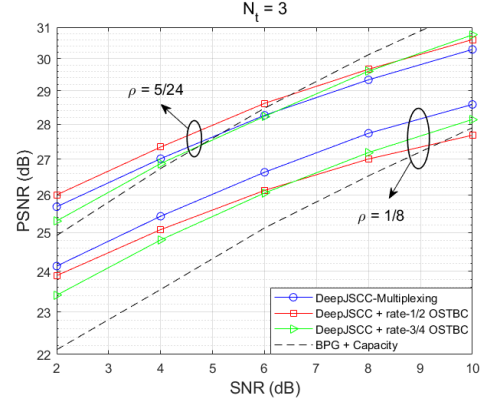


**Fig. 4:** The PSNR performance with  $N_t = 3$ ,  $N_r = 1$ , and bandwidth ratios,  $\rho = 1/8, 5/24$ .

$N_t > 2$  is too low to convey the underlying image; and hence, it is more beneficial to use the available antennas to improve the multiplexing gain. We highlight that given the 384 MIMO channel uses for  $\rho = 1/8$ , the length  $l$  of the latent vector  $\mathbf{z}$  for the multiplexing scheme is 1152; whereas it is  $l = 192$  and 288 for rate-1/2 and rate-3/4 OSTBC schemes, respectively, which are too small to achieve good reconstruction quality. On the other hand, when the available bandwidth ratio increases to  $\rho = 5/24$ , both diversity schemes can achieve comparable or better performance than the multiplexing scheme as  $l$  grows larger. We can also observe that the rate-1/2 OSTBC tends to perform better compared to the rate-3/4 one at lower SNR regimes which is intuitive as the rate-1/2 code provides higher diversity, and hence, higher reliability. Though OSTBC offers full diversity, the loss of bandwidth limits the overall end-to-end reconstruction performance when  $N_r > 1$ , which is not shown here due to page limitations.

## 5. CONCLUSION

In this paper, we presented novel DeepJSCC schemes for wireless image transmission over Rayleigh fading MIMO channels when CSI is available only at the receiver. In the diversity scheme, the user adopts OSTBCs to benefit from the full diversity offered by the multiple antennas. For the multiplexing scheme, the user directly maps the codewords to the transmit antennas and the residual assisted MMSE equalizer at the AP is used to estimate the transmitted codewords. Both schemes use end-to-end training to design the outer DeepJSCC encoder/decoder pairs. Simulation results show that with two transmit antennas, the diversity scheme outperforms the multiplexing scheme with lower system SNR and smaller number of receive antennas. We also show that the proposed system can outperform the ideal separation-based scheme adopting BPG algorithm delivered at the MIMO capacity. Exploring the end-to-end reconstruction performance of other diversity-multiplexing trade-off points and the data-driven selection among multiple OSTBCs will be considered in a future work.

## 6. REFERENCES

- [1] K. Sayood, H. H. Otu, and N. Demir, "Joint source/channel coding for variable length codes," *IEEE Transactions on Communications*, vol. 48, no. 5, pp. 787–794, 2000.
- [2] D. Gündüz, Z. Qin, I. E. Aguerri, H. S. Dhillon, Z. Yang, A. Yener, K. K. Wong, and C.-B. Chae, "Beyond transmitting bits: Context, semantics, and task-oriented communications," *arXiv:2207.09353*, 2022.
- [3] D. Gündüz, P. de Kerret, N. D. Sidiropoulos, D. Gesbert, C. R. Murthy, and M. van der Schaar, "Machine learning in the air," *IEEE Journal on Selected Areas in Communications*, vol. 37, no. 10, pp. 2184–2199, 2019.
- [4] Y. Shao, D. Gündüz, and S. C. Liew, "Federated learning with misaligned over-the-air computation," *IEEE Trans. Wireless Commun.*, vol. 21, no. 6, pp. 3951–3964, 2022.
- [5] N. Samuel, T. Diskin, and A. Wiesel, "Learning to detect," *IEEE Transactions on Signal Processing*, vol. 67, no. 10, pp. 2554–2564, 2019.
- [6] J. Ballé, V. Laparra, and E. P. Simoncelli, "End-to-end optimized image compression," in *5th International Conference on Learning Representations, ICLR 2017*.
- [7] N. Mital, E. Ozyilkan, A. Garjani, and D. Gündüz, "Neural distributed image compression with cross-attention feature alignment," *IEEE/CVF Winter Conf. on Applications of Computer Vision (WACV)*, 2022.
- [8] C. Bian, M. Yang, C.-W. Hsu, and H.-S. Kim, "Deep learning based near-orthogonal superposition code for short message transmission," in *ICC 2022*.
- [9] Y. Jiang, H. Kim, H. Asnani, S. Kannan, S. Oh, and P. Viswanath, "Turbo autoencoder: Deep learning based channel codes for point-to-point communication channels," in *NIPS*, 2019.
- [10] E. Ozfatura, Y. Shao, A. Perotti, B. Popovic, and D. Gündüz, "All you need is feedback: Communication with block attention feedback codes," *arXiv:2206.09457*, 2022.
- [11] E. Bourtsoulatze, D. B. Kurka, and D. Gündüz, "Deep joint source-channel coding for wireless image transmission," *IEEE Transactions on Cognitive Communications and Networking*, vol. 5, no. 3, pp. 567–579, 2019.
- [12] D. B. Kurka and D. Gündüz, "Deepjpsc-f: Deep joint source-channel coding of images with feedback," *IEEE Journal on Selected Areas in Information Theory*, 2020.
- [13] M. Yang, C. Bian, and H.-S. Kim, "Deep joint source channel coding for wireless image transmission with ofdm," in *ICC 2021 - IEEE International Conference on Communications*, 2021, pp. 1–6.
- [14] Y. Shao and D. Gündüz, "Semantic communications with discrete-time analog transmission: A PAPR perspective," *arXiv:2208.08342*, 2022.
- [15] H. Wu, Y. Shao, K. Mikołajczyk, and D. Gündüz, "Channel-adaptive wireless image transmission with OFDM," *IEEE Wireless Communications Letters*, 2022.
- [16] D. Gündüz and E. Erkip, "Joint source–channel codes for mimo block-fading channels," *IEEE Transactions on Information Theory*, vol. 54, no. 1, pp. 116–134, 2008.
- [17] L. Zheng and D.N.C. Tse, "Diversity and multiplexing: a fundamental tradeoff in multiple-antenna channels," *IEEE Transactions on Information Theory*, vol. 49, no. 5, pp. 1073–1096, 2003.
- [18] C. T. K. Ng, D. Gündüz, A. J. Goldsmith, and E. Erkip, "Distortion minimization in gaussian layered broadcast coding with successive refinement," *IEEE Transactions on Information Theory*, vol. 55, no. 11, pp. 5074–5086, 2009.
- [19] C. Bian, C.-W. Hsu, C. Lee, and H.-S. Kim, "Learning-based near-orthogonal superposition code for MIMO short message transmission," *arXiv preprint arXiv:2206.15065*, 2022.
- [20] W. Shi, J. Caballero, F. Huszar, J. Totz, A.P. Aitken, R. Bishop, D. Rueckert, and Z. Wang, "Real-time single image and video super-resolution using an efficient sub-pixel convolutional neural network," in *Proceedings of the IEEE Conference on Computer Vision and Pattern Recognition (CVPR)*, June 2016.
- [21] J. Xu, B. Ai, W. Chen, A. Yang, P. Sun, and M. Rodrigues, "Wireless image transmission using deep source channel coding with attention modules," *IEEE Transactions on Circuits and Systems for Video Technology*, vol. 32, no. 4, pp. 2315–2328, 2022.
- [22] V. Tarokh, H. Jafarkhani, and A.R. Calderbank, "Space-time block codes from orthogonal designs," *IEEE Transactions on Information Theory*, vol. 45, no. 5, pp. 1456–1467, 1999.
- [23] B. Hassibi and B.M. Hochwald, "High-rate codes that are linear in space and time," *IEEE Transactions on Information Theory*, vol. 48, no. 7, pp. 1804–1824, 2002.
- [24] S.M. Alamouti, "A simple transmit diversity technique for wireless communications," *IEEE J. Sele. Areas Commun.*, vol. 16, no. 8, pp. 1451–1458, 1998.
- [25] B. Hassibi and H. Vikalo, "On the sphere-decoding algorithm i. expected complexity," *IEEE Transactions on Signal Processing*, vol. 53, no. 8, pp. 2806–2818, 2005.